

Proceedings of the International Symposium on Physics of Materials (ISPMA 14), September 10–15, 2017, Prague

# An Integration of 3D Discrete Dislocation Dynamics with Numerical Tensile Testing

T. ZÁLEŽÁK<sup>a,\*</sup>, F. ŠIŠKA<sup>a</sup>, L. STRATIL<sup>a</sup>, S. FINTOVÁ<sup>b</sup>, V. HORNÍK<sup>b</sup>, D. BÁRTKOVÁ<sup>a</sup>,  
R. HUSÁK<sup>a</sup>, J. SVOBODA<sup>a</sup> AND A. DLOUHÝ<sup>b</sup>

<sup>a</sup>Institute of Physics of Materials, Academy of Sciences, Žižkova 22, 616 62 Brno, Czech Republic

<sup>b</sup>Institute of Physics of Materials (CEITEC IPM), Academy of Sciences, Žižkova 22, 616 62 Brno, Czech Republic

Design of materials for severe high temperature mechanical exposures can be assisted by a newly developed 3D discrete dislocation dynamics model which can be tailored for a numerical simulation of hot tensile tests. The 3D discrete dislocation dynamics model is based upon the linear theory of elasticity. The dislocation structure is represented by short straight segments. This allows a straightforward calculation of the stress fields and, subsequently, the driving forces at any point in the simulation cell as a linear sum of stress contributions of individual dislocation segments, osmotic forces, externally applied stress, misfit stresses, the Peierls stress etc. Furthermore, the model addresses interaction between dislocation segments and rigid incoherent spherical precipitates. The dislocation displacement is calculated from the equations of motion, which address both dislocation glide and climb. The external loadings enter the model as an applied strain during a tensile test, from which the resolved shear stress is calculated. The resolved shear stress is calculated from the Hooke law and it is constant throughout the simulated volume during one integration step. Furthermore, a benchmark study is performed in which the 3D discrete dislocation dynamics model of the tensile test focuses on a migration of a low angle dislocation boundary in a field of rigid spherical precipitates. Obtained results are compared to former calculations during which the applied stress was kept constant.

DOI: [10.12693/APhysPolA.134.779](https://doi.org/10.12693/APhysPolA.134.779)

PACS/topics: 61.72.Hh, 61.72.Lk, 62.20.Hg

## 1. Introduction

Material plasticity due to applied loadings is of a key importance for the material design and applications. The material response is mainly controlled by dislocation displacements, mostly through dislocation glide in low-index (compact) crystallographic planes. However, for high temperatures, non-compact glide (high-index planes) and dislocation climb due to thermally activated vacancy diffusion also has to be considered [1–3].

The material investigation covers a wide range of mechanical tests, among which we focus particularly on high temperature creep, which addresses a long-term material response to constant applied stress (or loading), and hot tensile tests performed at a constant strain rate. In the present contribution we apply a newly developed 3D discrete dislocation dynamics (DDD) model to precipitation hardened material, e.g. an oxide dispersion strengthened (ODS) alloy, subjected to the hot tensile test.

We investigate how a low-angle dislocation boundary passes an array of rigid incoherent spherical precipitates.

## 2. 3D DDD model

The presented model is based on the linear theory of elasticity [4]. The stress field due to the dislocation structure is evaluated in the approximation of short straight

segments of a general mixed character [3]. The total stress driving the dislocation system is then obtained as a linear combination of fields due the individual dislocation segments and the contribution from the externally applied stress [4]. The velocity of a dislocation segment, which, by integration, yields the segment displacement, is a linear function of the segment mobility and the Peach–Koehler force (PKF). The PKF is determined by the local stress field  $\hat{\sigma}$  and the line Burgers vector  $\mathbf{b}$  and the line direction  $\boldsymbol{\xi}$  [2, 4]:

$$\mathbf{f} = (\mathbf{b} \cdot \hat{\sigma}) \times \boldsymbol{\xi}, \quad (1)$$

The linearity of the PKF (Eq. (1)) allows a decomposition of  $\mathbf{f}$  into the edge and screw components

$$\begin{aligned} \mathbf{f} &= [(\mathbf{b}_e + \mathbf{b}_s) \cdot \hat{\sigma}] \times \boldsymbol{\xi} = (\mathbf{b}_e \cdot \hat{\sigma}) \times \boldsymbol{\xi} + (\mathbf{b}_s \cdot \hat{\sigma}) \times \boldsymbol{\xi} \\ &= \mathbf{f}_e + \mathbf{f}_s. \end{aligned} \quad (2)$$

Furthermore, the edge component can be projected to the glide plane and to the glide plane normal  $\mathbf{n}_g$ :

$$\mathbf{f}_e = \mathbf{f}_g + \mathbf{f}_c, \quad \mathbf{f}_g = [\mathbf{f}_e \cdot (\mathbf{n}_g \times \boldsymbol{\xi})] (\mathbf{n}_g \times \boldsymbol{\xi}),$$

$$\mathbf{f}_c = (\mathbf{f}_e \cdot \mathbf{n}_g) \mathbf{n}_g, \quad \mathbf{n}_g = (\boldsymbol{\xi} \times \mathbf{b}) / |\boldsymbol{\xi} \times \mathbf{b}|. \quad (3)$$

The velocity components are associated with the PKF components by the following relations:

$$\begin{aligned} v_g &= \frac{A_g f_g}{\sin \beta} \begin{pmatrix} \text{edge} \\ \text{glide} \end{pmatrix}, \quad v_c = \frac{A_c f_c}{\sin \beta} \begin{pmatrix} \text{edge} \\ \text{climb} \end{pmatrix}, \\ v_s &= \frac{A_s f_s}{\cos \beta} \text{(screw)}, \quad \cos \beta = \frac{\mathbf{b}}{|\mathbf{b}|} \cdot \boldsymbol{\xi}. \end{aligned} \quad (4)$$

\*corresponding author; e-mail: [zalezak@ipm.cz](mailto:zalezak@ipm.cz)

The velocity factors  $A_g$ ,  $A_c$  and  $A_s$  depend on the crystallographic orientation of the dislocation segments. For example, for the low-index glide, we put  $A_g = A_s = 10A_c$ , whereas for the non-compact glide, we put  $A_g = A_s = 2A_c$ . The climb factor is related to the thermally-activated vacancy diffusion

$$A_c = \frac{D_0 \Omega}{b^2 k T} \exp\left(-\frac{Q}{RT}\right), \quad (5)$$

where  $\Omega$  is an atomic volume,  $b$  is the length of Burgers vector,  $k$  is Boltzmann constant,  $R$  is gas constant,  $T$  is temperature,  $D_s = D_0 \exp(-Q/RT)$  is the factor of self-diffusion and  $Q$  is the activation energy of self-diffusion.

Let us introduce local coordinate system with  $xz$  plane coincident with the glide plane of the segment, the  $z$  axis oriented along the dislocation segment and the  $y$  axis represents the glide plane normal. Then the relations for the velocities of the edge and screw parts of the dislocation segments in local coordinates are

$$\mathbf{v}_e = (v_{e,x}, v_{e,y}, 0) = (v_g, v_c, 0), \quad \mathbf{v}_s = (v_{s,x}, v_{s,y}, 0). \quad (6)$$

The dynamics of the general mixed dislocation segments further obeys a thermodynamic extremal principle (TEP) [5], which yields [3]:

$$v_x = \frac{A_g A_s}{A_g \cos \beta + A_s \sin \beta} f_x, \quad v_y = \frac{A_c A_s}{A_c \cos \beta + A_s \sin \beta} f_y,$$

$$\mathbf{f} = (f_x, f_y, 0) \quad (\text{local coordinates}). \quad (7)$$

The 3D DDD model incorporates also rigid incoherent spherical precipitates. This means that the dislocations may not pass through the interface between the matrix and the precipitate. In the model, this is expressed by a reaction force, which is exerted by the precipitate on the dislocation in contact with the matrix-precipitate interface. The reaction force exactly compensates the driving force component normal to the interface. Applying the TEP, we obtain

$$f_p = -\frac{C_x f_x \cos \alpha + C_y f_y \sin \alpha}{C_x \cos^2 \alpha + C_y \sin^2 \alpha}, \quad \mathbf{f}_p = f_p (\cos \alpha, \sin \alpha, 0),$$

$$v = C_y (f_y + f_p \sin \alpha) / \cos \alpha, \quad \mathbf{v} = v (-\sin \alpha, \cos \alpha, 0). \quad (8)$$

The angle  $\alpha$  is delimited by the particle interface normal and the  $x$  axis of the local coordinate system associated with the segment. For further details on the 3D DDD model see [3, 6].

### 3. The numerical model of the tensile test

The total strain due to external loading can be decomposed into the elastic part and the plastic part. Here we first calculate a permanent strain due to a dislocation displacement in one particular glide plane.

We focus on a part of a crystal with dimensions  $l_x, l_y, l_z$  with a dislocation having a Burgers vector  $\mathbf{b} = \frac{1}{2}(b_x, 0, b_z)$  and line direction  $\xi = (0, 1, 0)$ . When a dislocation moves in the positive  $x$  direction, then a rectangle (solid line) depicted in Fig. 1, is deformed into a parallelepiped (dashed line). We have

$$\varepsilon_{xz}^p = \frac{1}{2} \left( \frac{b_x}{l_z} + \frac{b_z}{l_x} \right) = \frac{1}{2} \frac{b_x l_x l_y + b_z l_y l_z}{l_x l_y l_z} = \frac{1}{2} \frac{b_x \Delta S_z + b_z \Delta S_x}{V}, \quad (9)$$

where  $\Delta S_z = l_x l_y$ ,  $\Delta S_x = l_y l_z$  and  $V = l_x l_y l_z$ . The  $\varepsilon^p$  tensor represents a plastic contribution to the strain. For an arbitrary dislocation, this may be generalized as [7]:

$$\varepsilon_{ij}^p = \frac{(b_i n_j^{\Delta S} + b_j n_i^{\Delta S}) \Delta S}{2V}, \quad (10)$$

where  $\mathbf{n}^{\Delta S}$  is a unit normal vector to the plane element  $\Delta S$ .

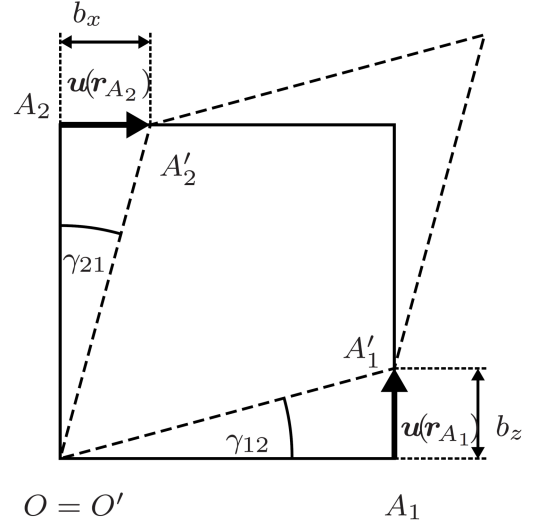


Fig. 1. Meaning of the shear components of the strain tensor;  $\mathbf{u}$  denotes the displacement.

The numerical tensile test uses the 3D DDD method to obtain plastic strain due to dislocation displacements. The total strain  $\hat{\varepsilon}$  is thus a superposition of the plastic strain  $\hat{\varepsilon}^p$  and the elastic strain  $\hat{\varepsilon}^e$ . To simulate a tensile test with a constant strain rate  $\dot{\hat{\varepsilon}}$ , we calculate these contributions in every iteration  $I$ :

$$\Delta \hat{\varepsilon}^{(I)} = \dot{\hat{\varepsilon}} \Delta t,$$

$$\Delta \varepsilon_{ij}^{p,(I)} = \sum_{s=1}^N \frac{(b_{s,i} n_{s,j}^{(I)} + b_{s,j} n_{s,i}^{(I)}) \Delta S_s^{(I)}}{2V}. \quad (11)$$

Here  $\Delta t$  is the time integration step,  $N$  is the number of dislocation segments,  $\mathbf{b}_s$  their Burgers vectors and  $\Delta S_s^{(I)}$  areas swept by these segments during the iteration  $I$ . The total strain  $\hat{\varepsilon}$  and total plastic strain accumulated up to the integration  $I$  are

$$\hat{\varepsilon}^{(I)} = \sum_{J \leq I} \Delta \hat{\varepsilon}^{(J)}, \quad \hat{\varepsilon}^{p,(I)} = \sum_{J \leq I} \Delta \hat{\varepsilon}^{p,(J)}. \quad (12)$$

The stress applied on the dislocation structure in the iteration  $I$  is obtained from the elastic strain in the iteration  $I$  using the Hooke law. Finally, the elastic strain and the associated stress in the iteration  $I$  is given by

$$\hat{\varepsilon}^{e,(I)} = \hat{\varepsilon}^{(I)} - \hat{\varepsilon}^{p,(I)},$$

$$\sigma_{ij}^{(I)} = 2\mu \varepsilon_{ij}^{e,(I)} + \frac{2\nu\mu}{1-2\nu} \delta_{ij} \varepsilon_{kk}^{e,(I)}. \quad (13)$$

#### 4. A migration of a low-angle tilt boundary during constant strain rate test

Following the earlier calculations [3, 6, 8, 9] where a low angle tilt boundary (LATB) was subjected to a constant shear loading, we have started with the same dislocation structure consisting of  $n$  initially parallel and equidistant edge dislocation lines in a basic simulation cell. The basic simulation cell contains a spherical particle and has two planes of symmetry  $y = 0$  and  $z = 0$ . Quasi-periodic boundary conditions involve a pattern composed of  $3 \times 3$  simulation cells (replicas of the basic simulation cell) along the  $y$  and  $z$  axes. The input parameters are summarized in Table I.

Input parameters of the model.

TABLE I

$\mu$	80 GPa	shear modulus
$\nu$	0.3	Poisson ratio
$D_0$	$2 \text{ cm}^2 \text{ s}^{-1}$	diffusion factor
$Q_4$	$240 \text{ kJ mol}^{-1}$	activation energy
$T$	873 K	temperature
$\Omega$	$(0.35 \text{ nm})^3$	atomic volume
$\mathbf{b}$	$(0.2, 0, 0) \text{ nm}$	Burgers vector
$\Delta t$	3 ms	time step
$\dot{\epsilon}_{xz}$	$1.25 \times 10^{-4} \text{ s}^{-1}$	constant strain rate
$N$	32	# of segments
$n$	$\{7, \dots, 17\}$	# of lines in a cell
$a_y; a_z$	200 nm	cell dimensions
$h$	$a_z / (n - 1)$	initial line spacing
$\mathbf{c}$	$[-50, 0, 0] \text{ nm}$	particle center
$d$	100 nm	particle diameter
$\lambda$	200 nm	particle distance
$l$	$\langle 3, 8 \rangle \text{ nm}$	segment length

In the presented calculations, a constant strain rate  $\dot{\epsilon}_{XZ}$  is applied without any initially applied stress, i.e.  $\hat{\sigma}^{(0)} = 0 \text{ MPa}$ . Thus in the very first integration step, the LATB does not move. As a result, after the first integration step, there is no plastic strain and the total strain  $\hat{\epsilon}^{(1)} = \hat{\epsilon} \Delta t$  is purely elastic. At the beginning of the second step,  $\hat{\sigma}^{(1)}$  is calculated from the Hooke law (Eq. (13)). The dislocations set in motion due to the nonzero applied stress and plastic deformation commences. With increasing time (increasing number of integration steps), the applied stress gradually increases up to the point when the LATB passes by the precipitate array.

The results obtained for different initial line spacings  $h$  are summarized in Fig. 2. The calculated stress-strain curve is shown in Fig. 2a, whereas the evolution of plastic strain with time is presented in Fig. 2b.

#### 5. Discussion

Our numerical results clearly show that the recent 3D DDD model [3] can be successfully extended to situations in which stresses due to the constant strain rate loading contribute to the driving forces which set dislocation

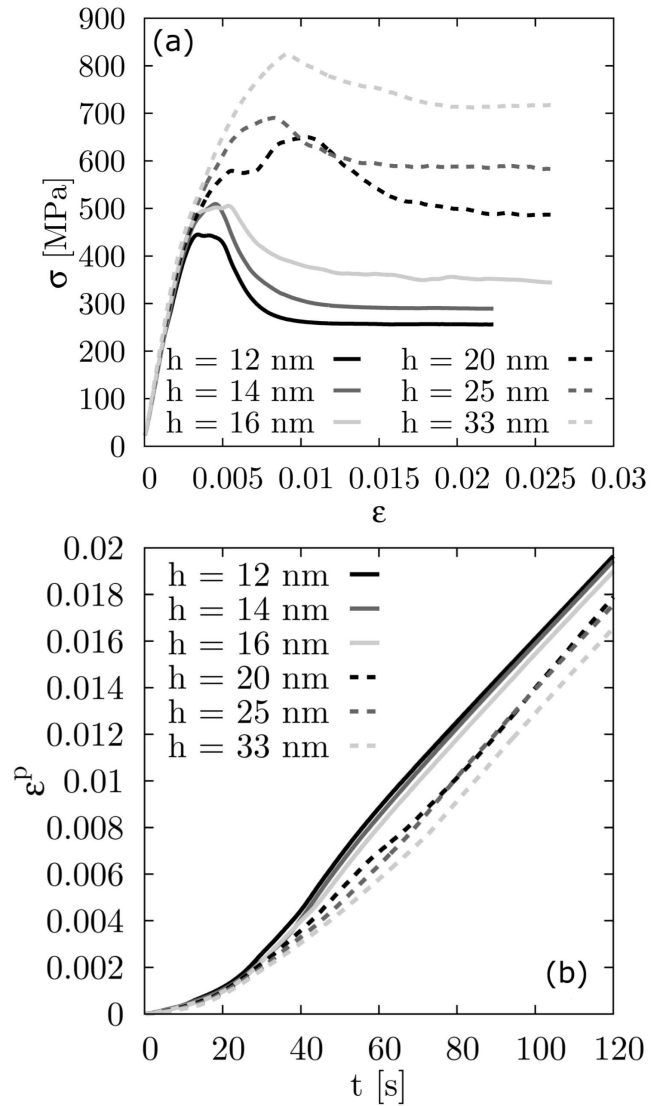


Fig. 2. (a) The stress-strain plot for the numerical constant strain test and (b) the plot of plastic strain contribution vs. time for  $\dot{\epsilon}_{xz} = 1.25 \times 10^{-4} \text{ s}^{-1}$  and 6 different initial line spacings  $h$ .

segments in motion. These simulations yield deformation curves similarly to stress-strain curves recorded in experiments. The numerical deformation curves (see Fig. 2a) start with a nearly linear part, where the plastic deformation is negligible. As the dislocation lines bow round the precipitates, the numerical curve deviates from the initial linear part. The imposed constant strain rate results in the increase of stress up to the point when the combined glide and climb motion of the dislocation segments in contact with precipitates makes the dislocation lines to pass by the precipitate array. From this moment on the plastic contribution to the overall strain outbalances the elastic strain and the stress decreases down to the level characteristic for the steady free motion of the LATBs (Fig. 2b).

Interestingly, our model shows that the values of the peak stress systematically decrease for denser LATBs (lower initial line spacings  $h$ ). This result reflects the fact that the total area swept by the dislocations for lower  $h$  (higher density of dislocations forming the LATB) is higher and thus also provides more plastic strain  $\hat{\epsilon}^p$ . While the total strain  $\hat{\epsilon}$  is imposed by the external loading condition and does not depend on the dislocation density, the elastic strain, which is a difference between the imposed total strain and the plastic strain, drops and yields correspondingly lower flow stress, see Eq. (13).

## 6. Summary and conclusion

We have extended our 3D discrete dynamics model [3] to situations where the total strain of the simulated system is externally imposed by the constant strain rate deformation. Under these conditions the calculations mimic a classical tensile test. The results suggest that denser dislocation boundaries can overcome particle arrays at lower flow stresses. The future development of the model will focus on a better representation of the stress-strain relation using finite element method (FEM). FEM-based calculations will allow better spatial resolution as far as the stress distribution in the calculation cell is concerned. However, even the preliminary results presented in this contribution provided an interesting and inspiring insight into the dislocation process governing the high temperature plasticity during hot tensile tests.

## Acknowledgments

The authors acknowledge the support from the Czech Science Foundation, project no 15-21292Y.

Additional financial resources for this work have also been provided by CEITEC (Central European Institute of Technology) due to a research infrastructure project no CZ.1.05/1.1.00/02.0068 financed by the European Regional Development Fund.

## References

- [1] J. Čadek, *Creep in Metallic Materials*, Elsevier, Amsterdam 1988.
- [2] D. Mordehai, E. Clouet, M. Fivel, M. Verdier, *Philos. Mag.* **88**, 899 (2008).
- [3] T. Zálezák, J. Svoboda, A. Dlouhý, *Int. J. Plast.* **97**, 1 (2017).
- [4] P. Hirth, J. Lothe, *Theory of Dislocations*, 2nd ed., Krieger, Malabar 1992.
- [5] F.D. Fischer, J. Svoboda, H. Petryk, *Acta Mater.* **67**, 1 (2014).
- [6] T. Zálezák, A. Dlouhý, *Acta Phys. Pol. A* **128**, 654 (2015).
- [7] V.V. Bulatov, W. Cai, *Computer Simulations of Dislocations*, Oxford University Press, 2006.
- [8] T. Zálezák, A. Dlouhý, *Acta Phys. Pol. A* **122**, 450 (2012).
- [9] T. Zálezák, *Ph.D. Thesis*, Masaryk University, Brno 2012.